Fermilab Library
0 1160 0052497 9

SDC-90-00083

DI
T

SDC
SOLENOIDAL DETECTOR NOTES

CONTRIBUTIONS OF ALBEDO AND NONCOMPENSATION TO CALORIMETER RESOLUTION

D. E. Groom

September 17, 1990

SDC-90-00083
17 September 1990
Snowmass '90 Contribution

CONTRIBUTIONS OF ALBEDO AND NONCOMPENSATION TO CALORIMETER RESOLUTION*

D. E. Groom
LBL 50-308, Berkeley CA 94720, USA

ABSTRACT

We have simulated the "intrinsic" resolution contributions of albedo loss and noncompensation in a large, homogenous calorimeter, using the cascade program FLUKA87. For a noncompensating calorimeter, the fluctuations in electromagnetic content via π^0 production produce a resolution contribution which is very nearly proportional to the degree of noncompensation and almost independent of energy—the so-called "constant term." For a lead calorimeter (essentially identical to a fine-sampling uranium-scintillator calorimeter), the constant term is approximately given by $14\% \times |1 - \epsilon_e/\epsilon_h|$, where ϵ_e/ϵ_h is nearly the "intrinsic e/h" introduced by Wigmans. Albedo losses produce a non-Gaussian contribution with $\sigma \approx 11\%/\sqrt{E}$, in reasonable agreement with experiment.

1. Introduction

As a step toward understanding calorimeter resolution, a study has been made in which only two irreduceable contributions exist: (a) "albedo" losses from the front face, and (b) fluctuations in the fraction of the energy going into the electromagnetic channel via π^0 production.

For simplicity, we choose a calorimeter which is "large," in the sense that no leakage occurs, and "homogenous," in the sense that there are no cracks and the absorber/readout-plane structure (if any) is the same from front to back. Cascades are simulated in a large lead cylinder, because lead has about the same density, radiation length, and nuclear interaction length as a fine-sampling uranium/scintillator calorimeter with uranium and scintillator plates of equal thickness.

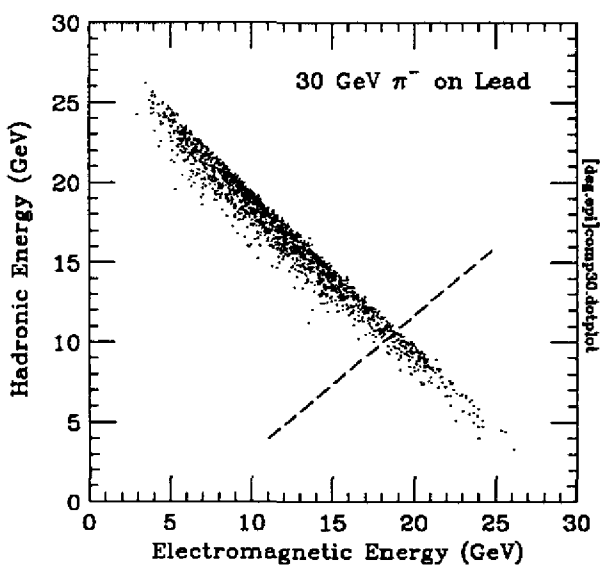

FIG. 1. Dotplot showing electromagnetic energy vs. hadronic energy deposition for cascades induced by 30 GeV/c π^- mesons normally incident on a large lead "calorimeter."

The general approach is illustrated in Fig. 1. Hadronic cascade events in the lead cylinder are simulated using FLUKA87[1]. For each event, the amount of energy deposited in electromagnetic and hadronic channels is recorded. For such an event the calorimeter response is

$$R_{\text{had}} = \epsilon_e E_{EM} + \epsilon_h E_{\text{had}} \ ,$$

where ϵ_e and ϵ_h are the efficiencies with which the calorimeter converts deposited electromagnetic and hadronic energy into an observable signal. The ratio ϵ_e/ϵ_h is very close to Wigmans' "intrinsic e/h," with qualifications discussed in Ref. 2. Given data like those shown in the dotplot, it is very easy to calculate resolution as a continuous function of the ratio ϵ_e/ϵ_h.

One can think of the measured distribution as the normal projection of the data onto the axis shown by the dashed line in Fig. 1. If the line makes a 45° angle with the x-axis, then electromagnetic and hadronic energies are weighted equally, and the calorimeter is compensating. In this case resolution is optimal. If the calorimeter is noncompensating, the projection axis is tilted,

* This work was supported by the Director, Office of Energy Research, Office of High Energy and Nuclear Physics, Division of High Energy Physics, of the U. S. Department of Energy under Contract No. DE-AC03-76SF00098.

and the scatter along the 45° line due to fluctuations in the π^0 content broadens the distribution.

Three effects contribute to the resolution:

a) The scatter along the 45° line due to π^0 content fluctuations, if the calorimeter is non-compensating;

b) Albedo losses from the front face, which show up in the figure as a non-Gaussian scatter away from the 45° line;

c) Failure of the program to exactly conserve energy on an event-to-event basis, which also shows up as scatter away from the 45° line.

Energy is lost in cases b) and c), and so events fall below the 45° line. The three effects are deconvoluted to separate the contributions at each energy.

2. Simulations

FLUKA is a high-energy hadronic cascade simulation code which transports particles down to a cutoff energy, set at 50 MeV for these runs. A switch can turn on EGS4. If the switch is off, as is the case here, the electromagnetic energy is deposited locally. All below-threshold hadronic energy is deposited locally.

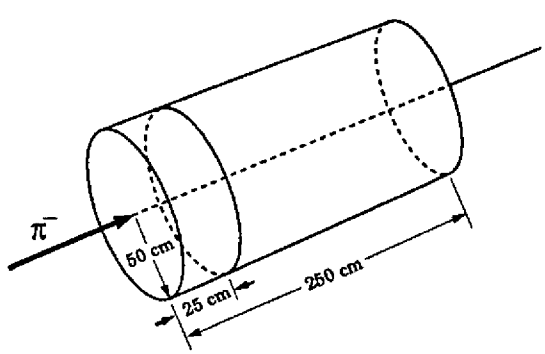

FIG. 2. Geometry of the lead cylinder used in the simulation runs.

The dimensions of the cylinder are shown in Fig. 2. For each energy, two runs are made: in one, pions incident along the axis are allowed to interact anywhere, and in the other, interactions are prohibited in the first 25 centimeters, or about 1.5 nuclear interaction lengths. In this case there is essentially no albedo loss. An example of data obtained with the interaction point constraint is shown in Fig. 3. The scatter normal to the diagonal is obviously much less than in Fig. 1.

One should expect all events to scatter along the 45° diagonal in the absence of albedo loss. A program has as much difficulty tallying all hadronic energy as does a real calorimeter, and most of the scatter perpendicular to the line is due to this problem. Newer versions of FLUKA have reportedly corrected the problem, but we have not yet rerun the simulations. The scatter is simply treated as another contribution to the resolution and removed by appropriate subtractions. Before analysis, the hadronic response at each energy is renormalized so that the resolution is optimized for $\epsilon_e/\epsilon_h = 1$.

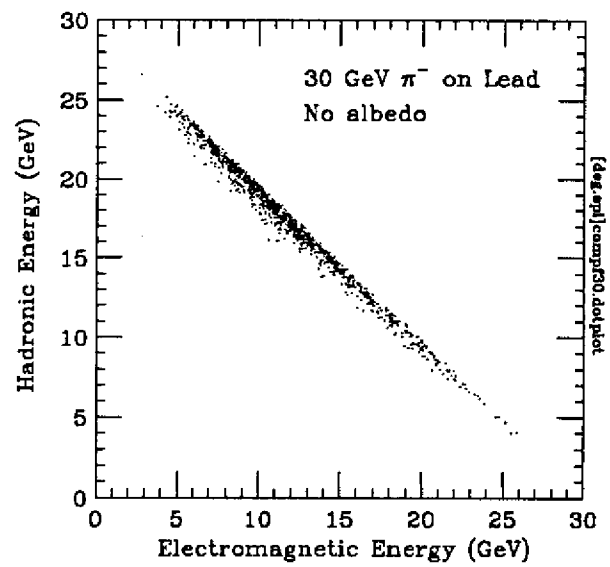

FIG. 3. As Fig. 1, except that the particles are constrained not to interact in the first 25 cm of the lead "calorimeter." Albedo losses are virtually eliminated.

3. Deconvolution

For a normal run (no constraint on the first interaction point) the net variance is taken as the sum of the three contributions discussed above:

$$\left(\frac{\sigma}{E}\right)^2_{\text{tot}} = \left(\frac{\sigma}{E}\right)^2_{\text{noncomp}} + \left(\frac{\sigma}{E}\right)^2_{\text{alb}} + \left(\frac{\sigma}{E}\right)^2_{\text{ext}}$$

The subscripts refer to the total resolution and contributions due to noncompensation, albedo loss, and the extraneous part due to energy nonconservation in the program. We use this approximation in spite of the fact that the

contributions (albedo in particular) are non-Gaussian. In the case of the constrained runs the albedo term is missing, and if we choose $\epsilon_e/\epsilon_h = 1$ the noncompensation term is also missing. Accordingly, all three contributions can be extracted from two runs at the same energy. Results of the procedure as applied to the data shown in Figs. 1 and 3 are shown in Fig. 4. It is interesting that (a) the non-

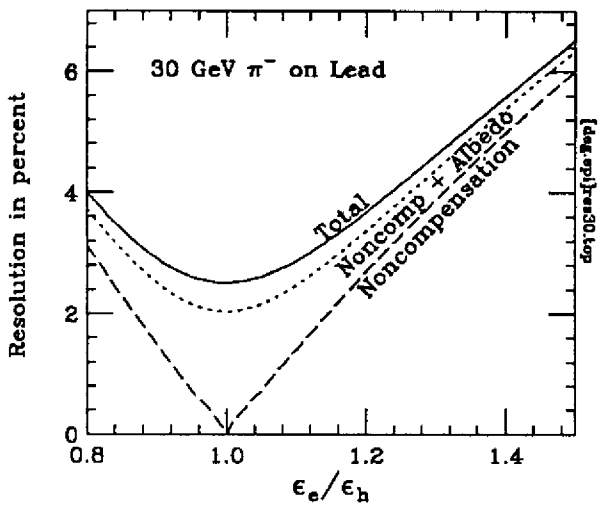

FIG. 4. Contributions to the resolution at 30 GeV as a function of the degree of noncompensation.

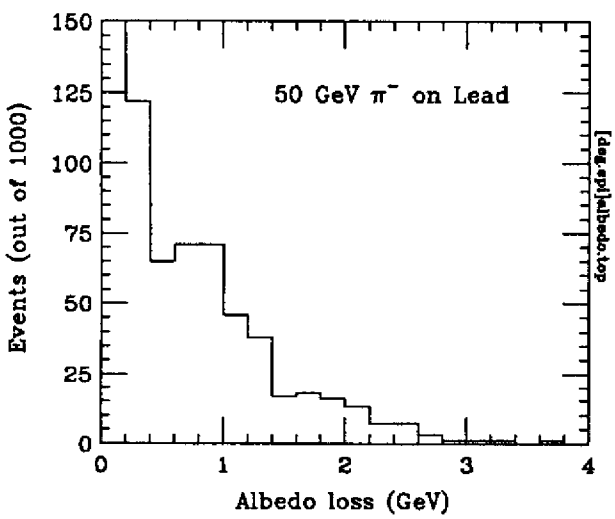

FIG. 5. Albedo loss spectrum for 1000 π^--induced cascades in lead. The first bin ($E <$ 0.2 GeV) contains 503 events. Since most of the escaping energy is carried by debris from the first few interactions, the amount of lost energy depends only weakly on incident energy.

compensation contribution is very nearly linear in the degree of noncompensation, $|1-\epsilon_e/\epsilon_h|$, and (b) albedo losses convert the intrinsic resolution into a hyperbola-like curve which is essentially flat within 10% of compensation. This is an energy-dependent statement, since the albedo contribution decreases with energy, while the noncompensation part stays almost constant.

The noncompensation contribution should be compared with that shown by Wigmans in Fig. 4 of Ref. 3. His slope is 22% $\times$ $|1-\epsilon_e/\epsilon_h|$, in contrast with our 14%, perhaps reflecting differences in the simulation programs and materials. The parabolic shape near the bottom is possibly the result of his (incorrect) direct addition of resolution contributions, rather than their addition in quadrature.

4. Results

A typical albedo-loss spectrum is shown in Fig. 5. At 50 GeV only half of the events lose more than 0.2 GeV. The distribution is quite skewed, since there can be very little albedo loss for events with first interactions deep in the calorimeter.

The particles escaping from the front of a calorimeter are produced in the first few hadronic collisions, and so the lost-energy fraction decreases as the energy of the incident hadron increases (as we shall see, as roughly $1/\sqrt{E}$). The scatter of points away from the 45° line in figures like Figs. 1 and 3 should therefore decrease with energy. In addition, the distributions shift to the right along the 45° line as the π^0 content increases with energy. These effects are shown in Fig. 6 for 500 GeV incident particles. The scatter along the 45° line must also decrease as the distribution moves to the right—in other words, the slope of the noncompensation contribution must decrease as the energy increases. In practice, this change is so small as to be lost in the Monte Carlo statistics. The resolution contribution due to fluctuations in the π^0 content is essentially constant, as has been pointed out by Wigmans.

These results are shown in Fig. 7, where we have evaluated the noncompensation contribution at $|1-\epsilon_e/\epsilon_h| = 0.1$.

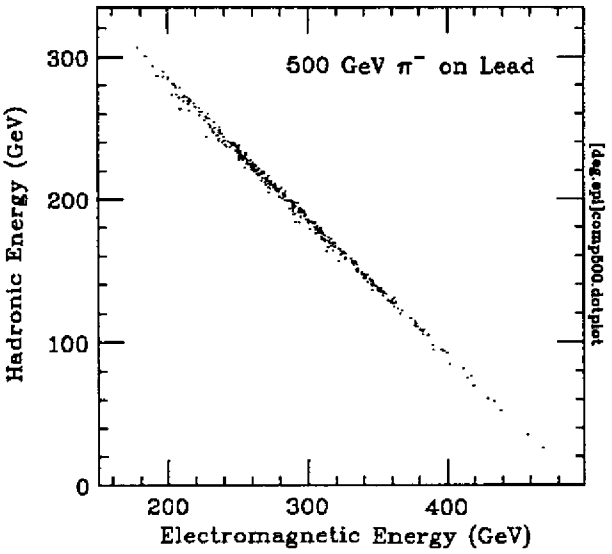

FIG. 6. Dotplot showing electromagnetic energy vs. hadronic energy deposition for cascades induced by 500 GeV/c π^- mesons normally incident on a large lead "calorimeter."

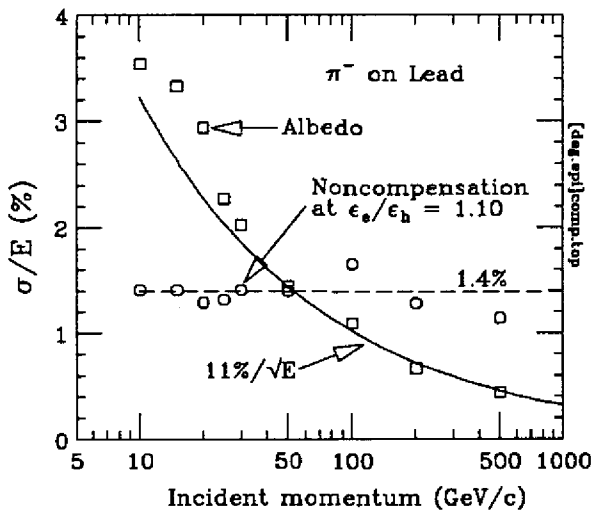

FIG. 7. Albedo loss and noncompensation contributions to resolution as a function of incident energy. The noncompensation contribution is evaluated at $|1-\epsilon_e/\epsilon_h| = 0.1$, and is nearly linear in $|1-\epsilon_e/\epsilon_h|$. Curves are drawn to guide the eye.

5. Comparison with experiment

The contributions of sampling and "intrinsic fluctuations" have been measured in a very nice series of test beam experiments by Drews *et al.*[4]. Lead/scintillator and uranium /scintillator test modules were exposed to electrons and hadrons with energies ranging from 10 GeV to 50 GeV. In some of the runs the plates were read out only on one edge, so that plates in even and odd positions provided two independent readouts. By summing and differencing the variances of different combinations of the two results, it was possible to separate the sampling and intrinsic fluctuations. Since sampling fluctuations dominated, errors on the intrinsic resolutions were fairly large. For hadrons incident on uranium/scintillator, the corrected result was $(20.4 \pm 2.4)\%/\sqrt{E}$, and for lead/scintillator it was $(13.4 \pm 4.7)\%/\sqrt{E}$. Both test calorimeters were nearly compensating, so a constant term is not expected.

The solid curve drawn in Fig. 7 is $11\%/\sqrt{E}$; it is not a fit because we did not attach errors to the Monte Carlo points. A somewhat higher curve would have been drawn for the range 10 GeV $< E <$ 50 GeV. In any case, it is difficult to assess which of the two experimental configurations is most closely modeled by our simulation in lead. The level of agreement does suggest that we have identified the energy-dependent intrinsic fluctuations extracted by Drews *et al.* with fluctuations in the front-face albedo losses. An experimental check would be straightforward: Events selected by requiring a near-minimum-ionizing signal in the first or second scintillator plane should exhibit no observable intrinsic fluctuations.

References

1. P. A. Aarnio, A. Fassò, H.-J. Möhring, J. Ranft and G. R. Stevenson, "FLUKA86 User's Guide," CERN TIS-RP/168 (1986);
   P. A. Aarnio, A. Fassò, J. Lindgren, J. Ranft and G. R. Stevenson, "Enhancements to the FLUKA86 Program (FLUKA87)," CERN TIS-RP/190 (1987).
2. D. E. Groom, "Energy Scaling of Low-Energy Neutron Yield, the e/π Ratio, and Hadronic Response in a Calorimeter," *Proc. of the Workshop on Calorimetry for the Superconducting Super Collider,* Tuscaloosa, Alabama, 13–17 March 1989, ed. R. Donaldson and M. G. D. Gilchriese, World Scientific (June 1990), 59–75.
3. R. Wigmans, Nucl. Instrum. Methods **A259**, 389 (1987).
4. G. Drews *et al.*, Nucl. Instrum. Methods **A290**, 335–345 (1990).